Near infrared avalanche photodiodes with bulk $Al_{0.04}Ga_{0.96}Sb$ and GaSb/AlSb superlattice gain layers

X-C. Cheng and T. C. McGill[a)]
Thomas J. Watson, Sr. Laboratory of Applied Physics, California Institute of Technology, Pasadena, California 91125

(Received 5 April 1999; accepted for publication 14 July 1999)

We demonstrate the use of bulk $Al_{0.04}Ga_{0.96}Sb$ and GaSb/AlSb superlattice as the gain material in a separate absorption/multiplication avalanche photodiode with sensitivity up to 1.74 μm. Both gain schemes were implemented in a molecular-beam epitaxy grown structure with a selectively doped InAs/AlSb superlattice as the *n*-type layer. Hole impact ionization enhancement was observed in $Al_{0.04}Ga_{0.96}Sb$ by using a two wavelength injection scheme. The superlattice gain layer device exhibited multiplication factors in excess of 300, and surface limited dark current at a level comparable to InGaAs/InAlAs devices of similar design. The superlattice gain layer was found to be more promising than its bulk counterpart due to its inherent lower dark current. © *1999 American Institute of Physics.* [S0021-8979(99)07620-3]

I. INTRODUCTION

There is much interest in making an AlGaSb avalanche photodiode with near infrared response as an alternative to the InP-based technology. Owing to the small band gap of GaSb, the long wavelength cutoff of such a device exceeds 1.7 μm and is well suited for communication purposes. With additional indium incorporation in the absorption region, the spectral response of GaSb can be extended out to 2.0 μm for niche applications such as night vision. Compared to rival InP/InGaAs devices, the antimonide photodiode has advantages due to its large ionization rates,[1] possible hole ionization enhancement from spin-orbit split-off band resonance,[3] and more potential in ionization enhancement from superlattice schemes[2] because of the large conduction band offset between GaSb and AlSb.

To date, there has been a number of studies on AlGaSb avalanche photodiodes, all of which have relied on liquid phase epitaxy (LPE) as the crystal growth method,[3–5] and focused on noise reduction from hole impact ionization enhancement when the spin-orbit split-off band difference Δ matched the band gap E_g in bulk AlGaSb. The results of these studies indicate a lack of consensus about the resonant hole ionization effect. There has been no investigation of antimonide avalanche photodiode with superlattice gain regions, whereas such schemes have already led to improved ionization ratios in the AlGaAs[6] and InGaAs[7] systems. In this article, we demonstrate that both bulk AlGaSb and GaSb/AlSb superlattice can be used as the gain medium in a structure fabricated from molecular-beam epitaxy (MBE), and draw direct comparison between the two different approaches.

II. STRUCTURE DESIGN, FABRICATION, AND CHARACTERIZATION

The device strictures were grown on GaSb substrates and consisted of a one-sided, abrupt p^-n^+ junction. As shown in Fig. 1, the unintentionally doped multiplication region was sandwiched between a heavily doped GaSb *p*-type ($p=2\times10^{18}/cm^3$) contact layer and a selectively doped InAs/AlSb superlattice. By incorporating Si only in the InAs constituent layer, the superlattice absorption layer was doped heavily *n* type ($n=1\times10^{18}/cm^3$) to minimize changes in depletion width and quantum efficiency at different reverse bias. The superlattice approach to *n*-type layer fabrication negated tellurium doping and allowed separate tuning of conduction and valence band edges[8] for band offset optimization. In a separate study reported elsewhere,[9] dark current suppression in this device structure was found to be critically dependent on the InAs/AlSb superlattice period and the resulting band offset Θ at the p^-n^+ heterojunction. Hence, an optimized design employing three stages of superlattice was adapted. The InAs layer was kept thin at 5 Å near the p^-n^+ interface to maximize Θ and suppress tunneling current across the junction. The structure was completed by a long period (27 Å) superlattice to lower the Schottky barrier at the surface and minimize contacting resistance.

The avalanche gain region consisted of either bulk AlGaSb or GaSb/AlSb superlattices. The Al concentration in the bulk gain layer was calibrated by using x-ray diffraction data and kept at 0.04. This is the composition at which the spin-orbit split-off band offset Δ equals the band gap E_g (Ref. 4) in AlGaSb, and possible hole ionization enhancement may occur. Due to the low vapor pressure of Sb, Ga tend to occupy Sb vacancies during AlGaSb crystal growth and form defects that are double acceptors. Hence, unintentionally doped AlGaSb is always *p* type. The background doping level of the $Al_{0.04}Ga_{0.96}Sb$ multiplication layer was determined to be $p=5\times10^{16}/cm^3$ from Hall measurements. For a one-sided abrupt *pn* junction, the reverse break down voltage V_B is given by[10]

$$V_B=60(E_g/1.1)^{3/2}(N_B/10^{16})^{-3/4},$$

where E_g is the room temperature band gap in electron volts, and N_B is the background doping in cubic centimeters. Given

a)Electronic mail: tcm@ssdp.caltech.edu

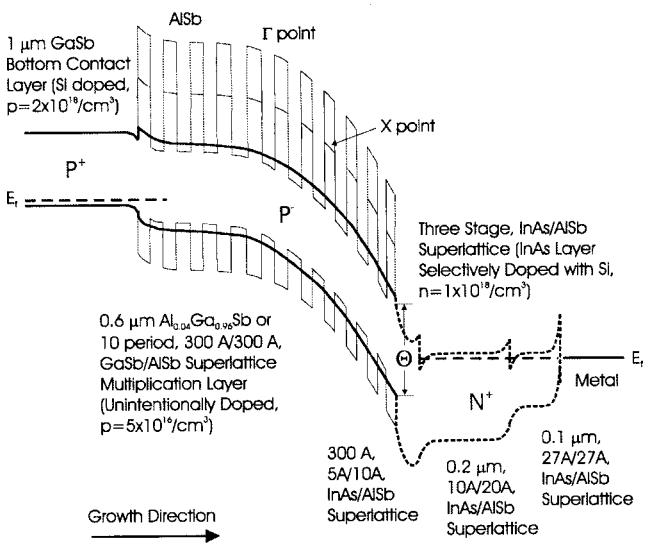

FIG. 1. Basic structure and band diagram of a separate absorption/multiplication antimonide avalanche photodiode grown by MBE. The device had a $p^- n^+$ configuration with a p^- $Al_{0.04}Ga_{0.96}Sb$ or GaSb/AlSb superlattice multiplication layer. The n^+ region consisted of three stages of selectively doped InAs/AlSb superlattice. The device is shown under reverse bias. The band gap of $Al_{0.04}Ga_{0.96}Sb$ is exaggerated for clarity.

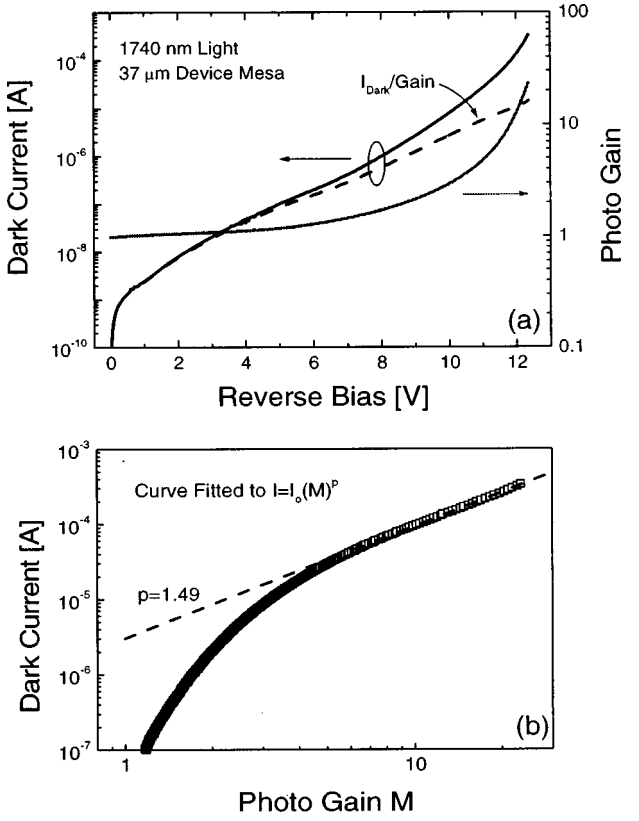

FIG. 2. (a) Dark current and near infrared photogain characteristics of avalanche photodiodes with $Al_{0.04}Ga_{0.96}Sb$ as the multiplication layer. The dashed line shows the unmultiplied dark current. (b) Device dark current plotted as a function of the photogain. The data was fitted to a power law $I=I_0(M)^p$, where $p=1$ for constant unmultiplied dark current.

the band gap of $Al_{0.04}Ga_{0.96}Sb$ at 0.75 eV, and the measured doping level, the bulk device was estimated to have an avalanche breakdown voltage of 14 V and a depletion width of 0.6 μm at breakdown. Thus, the $Al_{0.04}Ga_{0.96}Sb$ gain layer thickness was kept at 0.6 μm to maximize the length of the multiplication region.

The superlattice gain configuration consisted of ten periods of alternating GaSb and AlSb layers. The large conduction band offset (1.15 eV to the Γ point of AlSb, 0.55 eV to the *X* point of AlSb) and comparatively smaller valence band offset (0.45 eV) between these materials indicate a potential for electron ionization enhancement. For comparison purposes, the overall thickness of the GaSb/AlSb superlattice gain layer was kept the same as its bulk counterpart at 0.6 μm. This resulted in a GaSb or AlSb single layer thickness of 300 Å, which enabled ionizing carriers to gain enough energy at high field conditions ($E>10^5$/cm) to get out of the well.

Following epitaxial growth (the details of which is reported elsewhere),[9] devices were fabricated for direct injection of light into the semiconductor by employing a two step mask process. Since the InAs/AlSb superlattice contained both arsenides and antimonides, Cl_2 assisted dry etching was opted for the final mesa etch down. This was followed by a quick $C_4H_6O_6$:H_2O_2:HF(20:10:1) wet etch[11] to anneal out the surface damage. The resulting mesas ranged in size from 38 to 67 μm, and had a light sensitive circular opening surrounded by a ring of contact metal 2000 Å in thickness. The dark current of the avalanche photodiode was characterized by using a HP4156 parameter analyzer. The photogain characteristics were tested by using laser diodes of three different wavelengths (781, 1645, and 1740 nm). Light injection was achieved by butt coupling a single mode fiber (core diameter=9 μm) to the top surface of the device mesa. The 1645 and 1740 nm photons were absorbed in the underlying GaSb layer for electron injection and yielded essentially the same photogain curves, whereas 781 nm photons were absorbed in the *n*-type superlattice for hole injection. The optical sources were all chopped at 10 KHz.

III. DEVICE PERFORMANCE

A. Bulk $Al_{0.04}Ga_{0.96}Sb$ Multiplication Layer

Figure 2(a) shows the dark current and near infrared photogain characteristics of the $Al_{0.04}Ga_{0.96}Sb$ multiplication layer device. The device exhibited an avalanche break down voltage of 13 V, which was close to the predicted value of 14 V. The external quantum efficiency was 10% at zero bias. Maximum gains as high as 30 were observed. The dark current density was typically 6 A/cm^2 at a more moderate gain of ten. The device dark current level was comparable to LPE grown, bulk antimonide avalanche photodiodes of similar design.[12–14] However, it was much higher than the best leakage current in highly processed antimonide photodiodes (0.03 A/cm^2)[15] and also higher than the typical dark current found in InP-based avalanche photodiodes (0.5 A/cm^2 at a gain of ten).[16] We attribute this to lack of mature growth and processing technology for the antimonide avalanche photodiode and also the difference in device design, i.e., devices

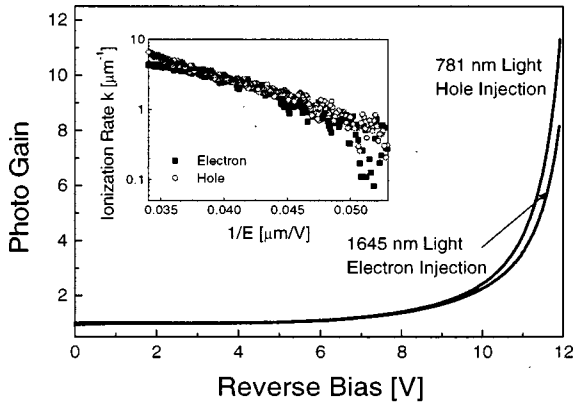

FIG. 3. Photogain curves for hole and electron injection using 781 and 1645 nm light (1740 nm light yielded the same result as 1645 nm light). Inset shows the calculated hole and electron impact ionization rates in $Al_{0.04}Ga_{0.96}Sb$. The field profile of an abrupt *pn* junction was assumed for the calculation.

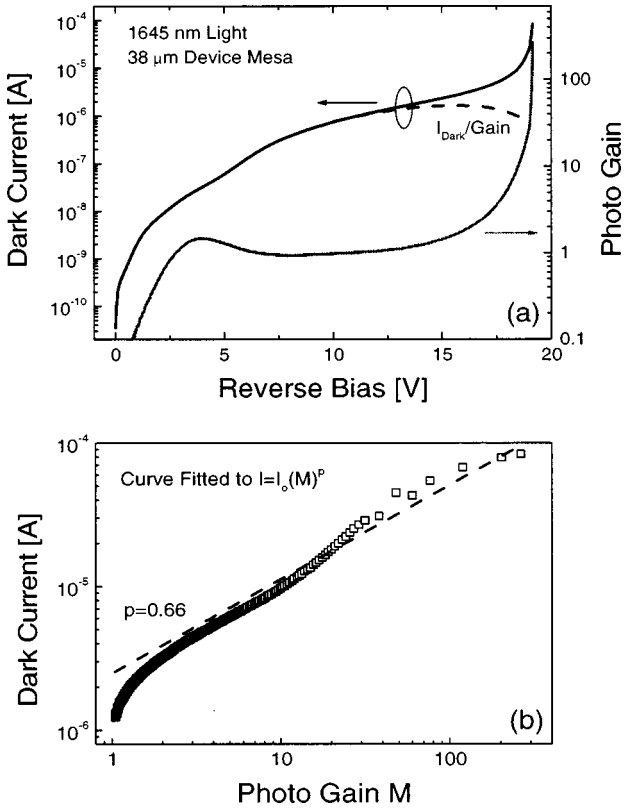

FIG. 4. (a) Dark current and photogain characteristics of avalanche photodiodes with a 10 period, 300/300 Å, GaSb/AlSb superlattice multiplication layer. The dashed line shows the unmultiplied dark current. (b) Device dark current plotted as a function of the photogain. The data was fitted to a power law $I=I_0(M)^p$, where $p=1$ for constant unmultiplied dark current.

intended for high speed applications have narrow, relatively highly doped multiplication regions and tend to have higher dark currents.

From Fig. 2(a), it can be seen that the dark current of the bulk $Al_{0.04}Ga_{0.96}Sb$ device increased exponentially with voltage at low bias. At high bias, the dark current deviated from the exponential curve due to additional avalanche gain. However, as shown by the dashed line in Fig. 2(a), the exponential behavior was recovered when the unmultiplied dark current, i.e., dark current divided by the photo gain, was plotted. This indicated that the reverse leakage was due mostly to bulk tunneling rather than surface leakage. The additional exponential contribution from tunneling accounted for the faster rise of the dark current compared to the photogain [Fig. 2(b)]. These observations were supported by scaling studies where the dark current was found to scale with the device area. Thus, we conclude that the relative high levels of dark current were due to band-to-band tunneling across the small band gap of the gain layer and were inherent to the bulk device.

The bulk device photo gain curves for 781 and 1645 nm light are shown in Fig. 3. Assuming separate carrier injections at these wavelengths, the ionization coefficients of electrons and holes can be derived from the photogain curves by using the formulas for a one-sided, abrupt junction without punch through[17]

$$k_n(E)=E\frac{1}{M_n(V)M_p(V)}\frac{dM_n(V)}{dV}$$

$$k_p(E)=E\left(\frac{1}{M_p(V)}\frac{dM_p(V)}{dV}-\frac{1}{M_n(V)}\frac{dM_n(V)}{dV}\right)+k_n(E),$$

where k_n and k_p are the electron and hole impact ionization rates, $M_n(V)$ and $M_p(V)$ the photogain at bias V for electron and hole injection, and E the maximum electric field in the abrupt *pn* junction at bias V. The calculated ionization rates are shown in the inset of Fig. 3 and can be seen to follow the expected $k=\exp(-a/bE)$ theoretical behavior.[18] However, the opening between the electron and hole curves was smaller than expected. We attribute this to mixed carrier injection due to absorption of 1645 nm photons by the InAs layers in the *n*-type superlattice and Franz–Keldysh absorption in the $Al_{0.04}Ga_{0.96}Sb$ multiplication layer. Additional deviation was caused by the slight increase in quantum efficiency at high reverse bias, as evidenced by the close proximity of the two photogain curves in Fig. 3 before reaching a nominal gain of two. Despite these short comings, the photogain curves in Fig. 3 clearly indicated hole ionization enhancement since higher gains were always obtained for hole injection. This result was highly reproducible and independent of incoming light intensity, injection geometry, or chopping frequency.

B. GaSb/AlSb Superlattice Multiplication Layer

The superlattice gain layer device yielded an avalanche break down voltage of 18.5 V. This was higher than its bulk counterpart due to the presence of additional AlSb barriers in the gain region. Since long wavelength photons were absorbed by GaSb layers in the superlattice gain region, only hole injection was achieved. There was little difference between the 781 and the 1645/1740 nm photogain curves except for the external quantum efficiencies achieved (20% and 5%, respectively). As shown in Fig. 4(a), gain factors up to 300 were observed in the near infrared. At a gain factor of 10, the dark current for the 37 μm device was 8 μA, yielding a nominal dark current density of 0.7 A/cm^2. This was an

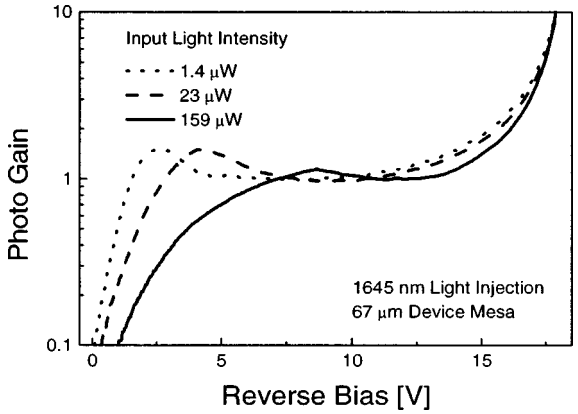

FIG. 5. Photo response of the GaSb/AlSb superlattice avalanche photodiode at different light intensity levels. The data was obtained by using a 1645 nm laser light. Similar results were obtained from 781 and 1740 nm light sources.

order of magnitude lower than in bulk $Al_{0.04}Ga_{0.96}Sb$ devices and comparable to InGaAs/InAlAs superlattice avalanche photodiodes of a similar design.[7] Although the observed dark current was higher than the best reported in the literature (0.02 A/cm^2 at a gain factor of ten from a flip chip bonded, InP-based, superlattice multiplication device),[19] the antimonide superlattice device remains promising because the dark current in the current device was limited by surface leakage, and hence, did not represent its fundamental limit. This is illustrated in Fig. 4. In contrast to the bulk device, it can be seen that the superlattice dark current increased slower than the photogain in the avalanche region [Fig. 4(b)]. In fact, the unmultiplied dark current stayed constant or decreased with voltage at high bias [dashed line in Fig. 4(a)]. This indicated that much of the dark current did not undergo multiplication and must be due to surface leakage. This result was supported by scaling studies were the dark current was found to scale with the device perimeter. To a large extent, the bulk tunneling current had been suppressed due to the presence of AlSb barriers in the superlattice gain region. With better processing and passivation techniques, the surface leakage can be readily reduced and device performance further improved.

It should also be noted that the superlattice gain layer exhibited characteristics significantly different from its bulk counterpart at low reverse bias. There was a strong dependence of collection efficiency on device bias due to the presence of AlSb barriers in the multiplication region. As shown in Fig. 5, a bias as high as 10 V was needed to overcome the barrier and reach unity gain. Moreover, a higher reverse bias was needed to achieve the same quantum efficiency as the input light intensity was increased. We attribute this effect to carrier trapping in the quantum wells in the multiplication region,[20] which tended to screen the applied electric field. A small negative resistance region was also observed in the photogain curve at low levels of light injection. Work is still in progress to understand this phenomenon.

IV. CONCLUSION

We have demonstrated the use of bulk AlGaSb and superlattice GaSb/AlSb gain layers in a MBE grown avalanche photodiode structure. The resulting devices had sensitivity in the near infrared up to 1.74 μm. Hole impact ionization enhancement was observed in bulk $Al_{0.04}Ga_{0.96}Sb$. However, this was accompanied by relatively high levels of dark current due to tunneling across the small band gap of the $Al_{0.04}Ga_{0.96}Sb$ multiplication layer. In comparison, GaSb/AlSb superlattice gain layers resulted in devices with much lower dark currents and more pronounced avalanche characteristics. This was attributed to suppression of bulk tunneling current by AlSb barriers in the gain region. The superlattice approach was deemed more promising because the observed dark current was limited by surface leakage and can be readily improved by using better processing and passivation techniques.

ACKNOWLEDGMENTS

The authors would like to thank A. T. Hunter and D. H. Chow of Hughes Research Lab for helpful discussion of antimonide growth and avalanche photodiode. This research was supported by the Defense Advanced Research Projects Agency and the Army Research Laboratory under Contract No. DAAL 01-97-K-0121.

[1] F. Osaka, T. Mikawa, and T. Kaneda, IEEE J. Quantum Electron. **OE−21**, 1326 (1985).
[2] G. F. Williams, F. Capasso, and W. T. Tsang, IEEE Electron Device Lett. **3**, 71 (1982).
[3] O. Hildebrand, W. Kuebart, K. W. Benz, and M. H. Pilkuhn, IEEE J. Quantum Electron. **OE−17**, 284 (1981).
[4] L. Gouskov, B. Orsal, M. Perotin, M. Karim, A. Sabir, P. Coudray, S. Kibeya, and H. Luquet, Appl. Phys. Lett. **60**, 3030 (1992).
[5] H. Kuwatsuka, T. Mikawa, S. Miura, N. Yasuoka, Y. Kito, T. Tanahashi, and O. Wada, Appl. Phys. Lett. **57**, 249 (1990).
[6] F. Capasso, W. T. Tsang, A. L. Hutchinson, and G. F. Williams, Appl. Phys. Lett. **40**, 38 (1982).
[7] T. Kagawa, Y. Kawamura, H. Asai, M. Naganuma, and O. Mikami, Appl. Phys. Lett. **66**, 993 (1989).
[8] D. H. Chow, Y. H. Zhang, R. H. Miles, and H. L. Dunlap, J. Cryst. Growth **150**, 879 (1995).
[9] X-C. Cheng and T. C. McGill, J. Cryst. Growth (to be published).
[10] S. M. Sze, *Physics of Semiconductor Devices* (Wiley, New York, 1981).
[11] P. S. Gladkov, Ts. Marinova, V. Krastev, and Sh. Dinkov, J. Electrochem. Soc. **142**, 2413 (1995).
[12] H. Kuwatsuka, T. Mikawa, S. Miura, N. Yasuoka, T. Tanahashi, and O. Wada, IEEE Photonics Technol. Lett. **PTL−2**, 54 (1990).
[13] H. Luquet, L. Gouskov, M. Perotin, A. Jean, A. Rjeb, T. Zarouri, and G. Bougnot, J. Appl. Phys. **60**, 3582 (1986).
[14] Y-M. Sun, J-M. Wang, and M-C. Wu, Jpn. J. Appl. Phys., Part 1 **35**, 5246 (1996).
[15] L. Gouskov, M. Perotin, G. Almuneau, and H. Luquet, J. Appl. Phys. **79**, 49 (1996).
[16] R. Ghin, J. P. R. David, S. A. Plimmer, M. Hopkinson, G. J. Rees, D. C. Herbert, and D. R. Wight, IEEE Trans. Electron Devices **45**, 2096 (1998).
[17] G. E. Stillman and C. M. Wolfe, in *Semiconductors and Semimetals*, edited by R. K. Willard and A. C. Beer (Academic, New York, 1977), Vol. 12.
[18] P. A. Wolff, Phys. Rev. **95**, 1415 (1954).
[19] I. Watanabe, S. Sugou, H. Ishikawa, T. Anan, K. Makita, M. Tsuji, and K. Taguchi, IEEE Photonics Technol. Lett. **5**, 675 (1993).
[20] R. E. Cavicchi, D. V. Lang, D. Gerhsoni, A. M. Sergent, H. Temkin, and M. B. Panish, Phys. Rev. B **38**, 13474 (1988).